

Study of a 20 kHz power ultrasound field in presence of an external liquid flow: application to in-situ boat hull cleaning

MAZUE Gérald^{a,b}, VIENNET Rémy^{b*}, HHHN Jean-Yves^b, BONNET Dimitri^{b,c}, BARTHES Magali^c,
BAILLY Yannick^c, ALBAÏNA Ignaki^a

^a Navyclean

Traverse Collet Redon, 13013 Marseille, France

^b Institut UTINAM (UMR UFC/CNRS 6213)

30 Avenue de l'Observatoire, 25000 Besançon, France

^c Institut FEMTO-ST (UMR UFC/CNRS 6174)

2 Avenue Jean Moulin, 90000 Belfort Cedex, France

Abstract

This work is part of a project consisting in the development of an automatic cleaning station for the immersed part of boats. This self-service station combines ultrasound for washing with a specific water treatment. In this case, displacement of the transducers plus suction of the dirt removed induce circulation, and we need to measure the ultrasound activity which reaches the surface despite the disruptions. The goal of this work is to quantify this ultrasound activity. Two methods were implemented for this quantification: Particle Image Velocimetry and electrochemical mass transfer measurements.

Key words: Cleaning, Ultrasound, PIV, hydrodynamics, electrochemistry.

Nomenclature

| | | |
|-----------|---|------------------------------------|
| V_p | Tangential equivalent velocity determined from electrochemical measurements | [m.s ⁻¹] |
| U | Mean velocity in the section of the test cell, calculated from flow rate values | [m.s ⁻¹] |
| U_{PIV} | Spatial mean velocity on the ROI, calculated from PIV values | [m.s ⁻¹] |
| ROI | Region of interest | |
| D | Diffusion coefficient | [m ² .s ⁻¹] |
| C_{sol} | Concentration of the electroactive species | [mol.m ⁻³] |
| ν | Kinematic viscosity | [m ² .s ⁻¹] |
| n | Number of electrons transferred | |
| d | Electrode diameter | [m] |
| F | Faraday number | [C.mol ⁻¹] |
| j_D | Current density | [A.m ⁻²] |
| x | Length | [m] |

1. Introduction

In practice, cleaning of a boat hull requires removal of the boat from the water. This operation is rather expensive, and the boat remains stationary for at least two days. Cleaning is usually performed using high pressure water. This procedure is completed by applying a layer of antifouling paint, which, while slowing down dirt deposition, is also a well-known source of chronic pollution. This paintwork is efficient for about one year, and the dirt layer remains thin and virtually not adhesive. After a while, however, the layer becomes more adhesive and leads to a decrease in boat performance. To keep a hull in good condition, it must be cleaned once a year; otherwise, use of more extensive operations (such as sandblasting, etching, etc.) will be necessary.

The effectiveness of ultrasound in cleaning processes has been proved in a large number of industrial applications such as extraction (Araujo et al., 2013) and emulsification (Abismail et al., 1999). Moreover, the cavitation phenomenon, induced by ultrasound in the liquid media, acts as a mechanical cleaning tool. Indeed, some bubbles collapse asymmetrically near the surface (Compton et al., 1994; Krefting et al., 2004), inducing a high velocity liquid jet on the surface.

Use of ultrasound thus appeared promising for designing a new automatic cleaning station for immersed boats, the design of which has already been presented (Mazue et al., 2011). The cleaning tool in question consisted of 3 transducers operating simultaneously at 20 kHz and moving along the surface. Two suction holes collected the dirt removed from the hull. The complete mechanical tool is able to absorb boat movement during the cleaning process. To obtain an acoustic activity high enough to allow efficient boat hull cleaning, specific wave guides were designed, made of titanium alloy (TA6V) to resist corrosion in marine environments. Each transducer associated with its specific wave guide was sealed in a tight housing to avoid power loss and electric shocks. Ultrasound devices were also calibrated using calorimetry or Fricke dosimetry methods, mass transfer measurements and sonoluminescence visualization.

Knowledge of the location of the more active zones is an important criterion in optimization of ultrasound effects. Thus, different methods were developed in order to visualize the active zones in a media. The most widely used methods are sonoluminescence (Gondrexon et al., 1995), mass transfer measurements (Trabelsi et al., 1996) or laser visualizations (Tomography (Mandroyan et al. 2009a), and Particles Image Velocimetry (Mandroyan et al. 2009b)). According to the papers available in the literature, these techniques were carried out in motionless liquid bulk. Nevertheless, many large-scale applications actually involved additional liquid circulation inside the acoustic field. With respect to ship hull cleaning, both displacement of the transducers and suction of the dirt removed induce this additional circulation. We thus need to quantify the ultrasound activity which reaches the surface despite the disruptions due to the additional flow.

Two measurement methods are relevant with a view to provide useful information concerning influence of a liquid flow perpendicular to wave propagation. The first method consists of the electrochemical measurements of mass transfer phenomena by cyclic voltametry using the well-known quasi-reversible redox couple $\text{Fe}(\text{CN})_6^{3-} / \text{Fe}(\text{CN})_6^{4-}$. The second method is Particle Image Velocimetry (PIV) for velocity vector field determination. The latter is a laser-based method. When applying cross-correlations between two successive pictures of a particle seeded flow, the PIV process ensures a 2D velocity field in a flow plane (Raffel et al. 1998). It was proved that the main contribution of stirring at the electrode surface facing the ultrasonic horn accounts for as much as 90% from asymmetric cavitation (Hihn et al., 2011). Mass transfer measurements focus on parietal phenomena and thus emphasize the influence of perpendicular circulation. On the other hand, PIV describes global bulk motion and, more precisely, convective motion. It focuses on the “ultrasonic wind” (Pollet et al., 2007; Hihn et al., 2011) and how the latter will be disturbed by the additional liquid circulation.

2. Experimental setup

A specific setup, consisting of a cross-section polypropylene measurement cell (40 mm x 35 mm height, 400 mm length) was designed (figure 1). Both the ultrasound probe and the electrode (used for mass transfer measurements) were embedded in a flange. Whereas the ultrasound probe was fixed at the bottom, the working electrode was located at the top of the cell, facing the transducer center. For laser visualization, both the front and top windows were made of PMMA. A centrifugal pump supplied a controlled flow ($0 < \text{Reynolds} < 50000$), which could be adjusted via a by-pass system. The liquid was stored in a 25 L thermostatic tank.

All experiments at 20 kHz were conducted using a 25 mm diameter titanium probe (Sonics&Material, Danbury, USA). For mass transfer measurements, a 1 mm platinum disk embedded in a glass tube was located on a surface opposite the transducer. This electrode was polished down to $1/4 \mu\text{m}$ granulometry. The quasi reference electrode was a platinum wire, and the counter electrode consisted of a platinum

crowns designed and located so as to be outside the ultrasonic field. The liquid solution was potassium ferri/ferrocyanide ($5 \cdot 10^{-3} \text{ mol.L}^{-1}$) in sodium hydroxide (0.2 mol.L^{-1}). Mass transfer measurements under sonication were taken using the electrodiffusion method with the redox couple $\text{Fe(CN)}_6^{3-}/\text{Fe(CN)}_6^{4-}$. Voltammograms of the ferri-ferrocyanide reversible couple were recorded, and the mass transfer coefficient (k_d) was calculated using the value of the limited current corresponding to a signal plateau. Stirring at the electrode surface was quantified by electrochemical measurements and quoted as the “equivalent” flow velocity (Pollet et al., 2007), which represents global streaming at the electrode surface.

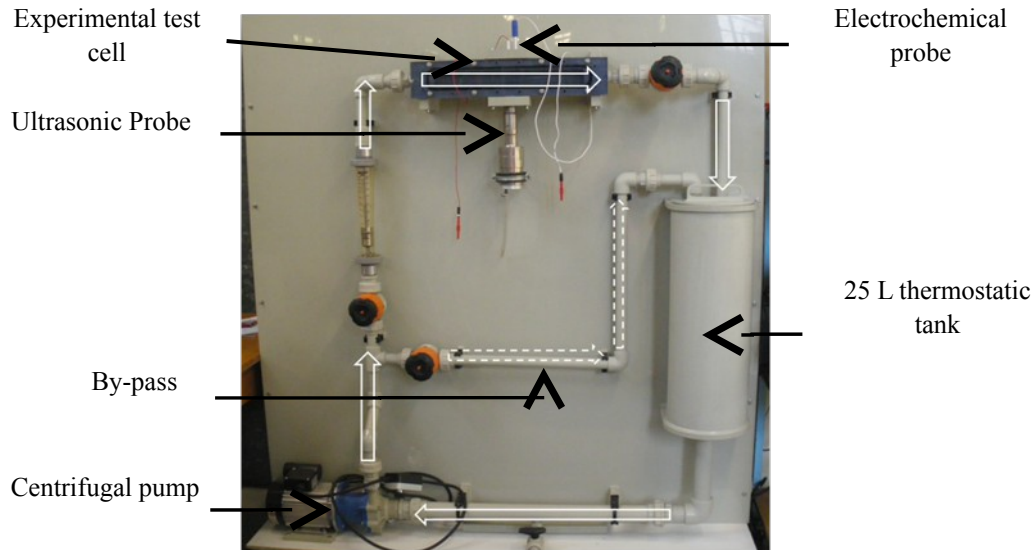


Figure 1. Experimental setup

In the specific case of a tangential flow to the electrode surface, another equivalent velocity, V_p , can be defined. This corresponds to the value that axial velocity should reach to obtain similar electrochemical measurements in silent conditions (without ultrasound). This parietal equivalent velocity is given by the following equation (Mazue et al., 2013):

$$V_p = \frac{1}{(0,6 nFC_{sol})^2} \cdot D^{-4/3} \cdot v^{1/3} \cdot j_D^2 \cdot d^{2/3} \cdot x^{1/3} \quad (1)$$

In this case, x represents the distance between the center of the electrode and the start of the diffusion layer (see Mazue et al., 2013).

For PIV measurements in the liquid loop, we used a dual beam pulsed Nd:YAG laser (532 nm). The optical setup used is presented in figure 1. The laser beam was spread as a laser sheet by means of optical components (cylindrical and spherical lenses), and redirected toward the liquid flow by a prism. The camera (PIVCAM 13-8, 12 bits) and the laser were triggered by a synchronizer. The liquid flow was seeded with hollow glass beads (8 to 12 μm in diameter).

Two laser beams were flashed at a given frequency. For each flash, an image of the flow was recorded by the camera. The time separating the two images (known as pulse delay Δt) was set at 100 ms or 300 ms (depending on the operating conditions). For each operating condition, 100 pairs of images were recorded. The pump’s vibrations were responsible for relative displacement between two successive pairs of images, meaning that images did not have the same spatial origin. To correct images, the relative displacement was calculated using the classical PIV correlation process. Images were then translated of the displacement’s value and saved. This pre-processing was achieved using the PYV software developed at the Femto-ST institute (Bonnet et al. 2011; Bonnet et al. 2012). This software was also used to select various ROI, to correct image orientation (rotate and flip operations to place images in the main flow direction), and to apply different full PIV processing on each ROI. In this experiment, the selected ROI (1024 x 1056 pixels) corresponded to the whole visualization area (Figure 2). The cross-correlation PIV process on the ROI delivered instantaneous velocity vector fields. A second correlation peak filtering

eliminated aberrant velocity vectors. Out of the 100 vector fields obtained for each operating condition, one mean vector field was calculated. On the selected ROI or on a specific area, spatial mean velocities were also calculated.

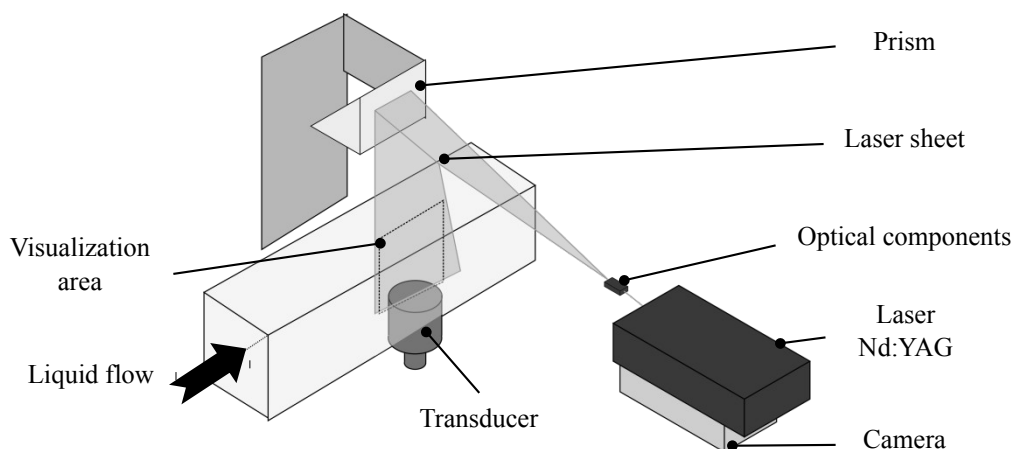


Figure2. Optical setup for PIV measurements

3. Results and discussions

The present experimental setup and the two measurement methods, presented in the previous section, allowed us to visualize and identify perturbation of the acoustic field due to presence of the additional liquid flow. The cavitation phenomenon in the liquid media, induced by ultrasound, plays a preponderant role in cleaning ultrasound applications. In the present case, we need to verify whether ultrasound effectiveness is disturbed by the additional flow motion between the cleaning surface and the transducer. In a first step, parietal velocities V_p were calculated from electrochemical data. Then, from PIV measurements, we obtained velocity vector fields throughout the observation window, from which a spatial average velocity U_{PIV} was calculated. Both V_p and U_{PIV} are shown versus the Reynolds number, and then compared with U , the theoretical mean velocity in the section of the test cell calculated from the flow rate values (Figure 3).

This figure shows that all three curves are very similar. This result enables us to validate use of the parietal velocity V_p calculated from mass transfer measurements. Likewise, it shows that use of the PIV method is relevant since it also provides a good estimation of liquid circulation velocity.

In a second step, the same kind of experiment was carried out, this time in the presence of an ultrasonic field provided by a 20 kHz transducer. Both electrochemical and PIV measurements were used to evaluate the disturbance induced by the additional liquid flow on the ultrasound field. Spatial average velocities U_{PIV} were always higher in the presence of ultrasound than in silent conditions (see figure 4). Furthermore, the difference between U_{PIV} with and without ultrasound tended to decrease steadily as the Reynolds number increased. When the Reynolds number reached values higher than 7000, the two velocities were almost the same, and ultrasound influence seemed less marked. This result was confirmed by the velocity vector fields obtained by PIV and shown in figure 5. These pictures showed, for three different values of the Reynolds number, the deviation of the convective flow induced by the ultrasound field. This deviation is attributed to the additional perpendicular fluid circulation. For the highest forced liquid flows (i.e. for $Re > 7000$), the convective flow plume was pushed out of the observation window and the detection by PIV of the influence of ultrasound became negligible.

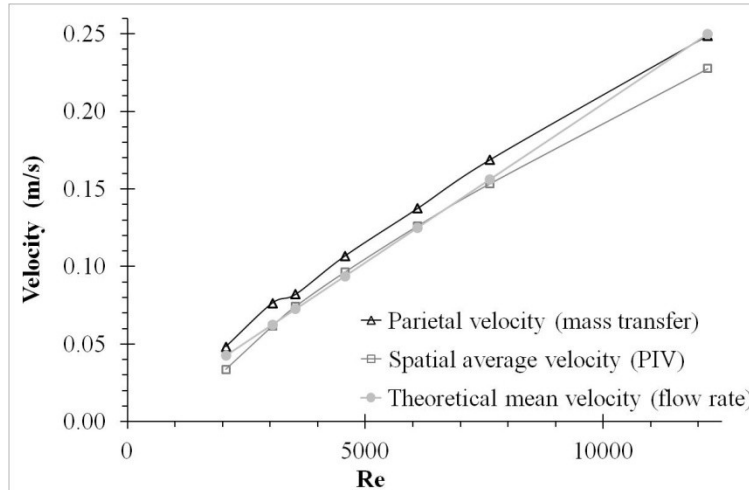


Figure 3. Comparison of the velocity values in silent conditions obtained from mass transfer (parietal velocity V_p), PIV (spatial average velocity U_{PIV}) and flow rate measurements (theoretical mean velocity U).

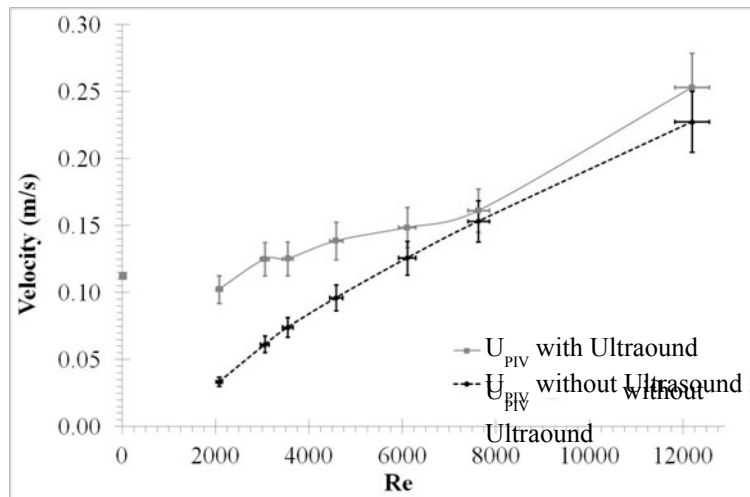


Figure 4. Evolution with the Reynolds number of the spatial average velocities U_{PIV} , with and without ultrasound, obtained from PIV measurements. Average calculated throughout the visualization area.

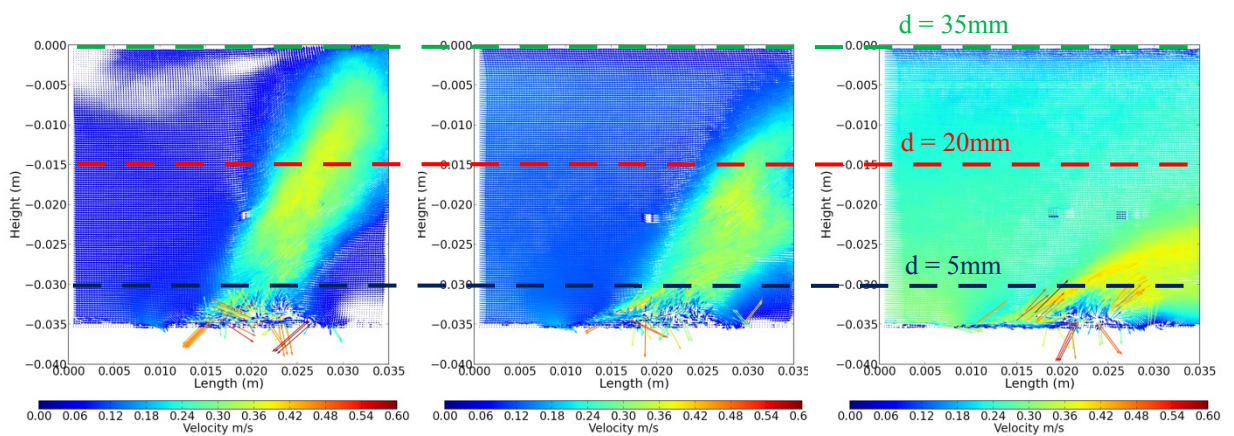


Figure 5. Velocity vector fields obtained by PIV, in the presence of an acoustic field (20 kHz) and for three different Reynolds numbers: 3500 (on the left), 7600 (middle), 12200 (on the right).

We compared the results obtained by PIV with those obtained by electrochemical measurements. Figure 6 shows equivalent parietal velocities V_p and spatial average velocities U_{PIV} obtained with and without ultrasound. V_p was always greater in ultrasound presence than in silent conditions. Moreover, V_p with ultrasound was always greater than U_{PIV} . Moreover, for the highest Reynolds number ($Re > 7000$), U_{PIV} values were almost of the same order of magnitude with and without ultrasound. On the contrary, for $Re > 7000$, V_p values in the presence of ultrasound remained higher than the three other velocities (U_{PIV} with and without ultrasound, V_p without ultrasound). Thus, even if the convective flow plume was completely pushed out of the measurement window (see figure 5), a part of the acoustic energy still reached the wall opposite the transducer. This result seemed to corroborate what we mentioned earlier in the introduction: the main contribution of stirring at the electrode surface facing the ultrasonic horn accounts for as much as 90% from asymmetric cavitation (Hihn et al., 2011). This last result was very important in our case since it confirmed that, even in a highly disturbed hydrodynamic environment, ultrasound remained effective on the wall opposite the transducer.

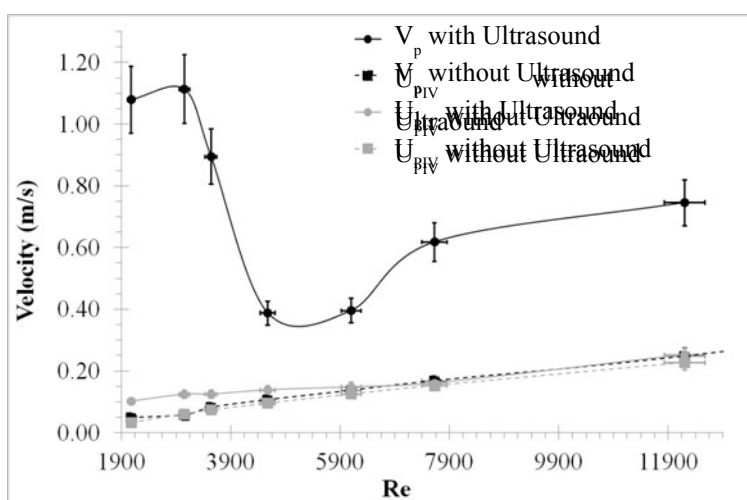


Figure 6. Comparison of parietal equivalent velocity V_p (electrochemical measurements) and spatial average velocity throughout the visualization area U_{PIV} (PIV measurements) with and without ultrasound.

These results were obtained for a distance of 3.5 cm between the transducer and the opposite wall on which the electrochemical probe was located. However, for our boat cleaning application, the distance between the transducers and the surface to be cleaned must be less than 1cm. We thus carried out experiments to emphasize the influence of transducer/working electrode distance on V_p values. The working electrode was located at various heights in the experimental test cell. With and without ultrasound and for three flow rates (15, 24 and 120 $L \cdot min^{-1}$), V_p values were calculated for different transducer/working electrode distances (from 5 mm to 35 mm). Previous studies (Mandroyan et al., 2009a, b) well described this zone in static conditions, which corresponds to half a wavelength at 20 kHz.

Results are presented in table 1. The transmitted ultrasound power was determined with calorimetric measurements. In the vicinity of the electrode, no significant impact on global stirring was reported due to the additional perpendicular liquid circulation. On the contrary, the combination of ultrasound and flow rate improved the global effect near the surface. Thus, the presence of a flow rate did not entail a loss of cleaning efficiency, particularly for shorter distances. This last result seemed predictable from the PIV velocity vector fields in figure 5. Indeed, on these images, we virtually marked three positions of the electrochemical probe. Even if the velocity field would not be exactly the same with the electrode inside the additional flow, we can see from the plume's deviation that, for small distances, acoustic streaming

would be efficient. Thus, even in the case of highly distorted hydrodynamics, the boat hull cleaning by ultrasound should be relevant.

Table 1: V_p calculated for different transducer/electrode distances, with and without ultrasound and for three different flow rates.

| Transmitted Power (W) | Re $\pm 4\%$ | Flow rate (L/mn) | Parietal equivalent velocity V_p (m.s ⁻¹) $\pm 10\%$ | | | | | | |
|-----------------------|--------------|------------------|--|---------|---------|---------|---------|---------|---------|
| | | | d=5 mm | d=10 mm | d=15 mm | d=20 mm | d=25 mm | d=30 mm | d=35 mm |
| 0 | 7600 | 15 | 0.09 | 0.14 | 0.19 | 0.16 | 0.11 | 0.11 | 0.07 |
| | 12200 | 24 | 0.27 | 0.30 | 0.32 | 0.31 | 0.30 | 0.23 | 0.16 |
| | 61000 | 120 | 2.61 | 2.70 | 2.91 | 2.36 | 2.49 | 2.06 | 2.17 |
| 51 | 7600 | 15 | 11.08 | 7.88 | 5.35 | 3.40 | 2.70 | 2.02 | 0.91 |
| | 12200 | 24 | 8.16 | 4.80 | 6.12 | 3.08 | 4.55 | 2.58 | 1.56 |
| | 61000 | 120 | 21.77 | 11.78 | 7.14 | 5.82 | 4.70 | 5.01 | 4.40 |

4. Conclusions

This study highlighted several interesting results. Both PIV and electrochemical mass transfer measurements, implemented in this work, provided relevant information concerning interactions between the ultrasonic field and perpendicular fluid circulation. First, a study without ultrasound showed that calculation of an equivalent velocity with electrochemical mass transfer measurement yielded a good estimation of flow velocity, and was useful for comparison with PIV average velocity determination. Secondly, when ultrasound was added, even if the convective flow induced by the acoustic field was completely deviated by perpendicular flow circulation, ultrasound contribution remained noticeable on the surface opposite the transducer. This last result was of prime importance for the cleaning application.

References

- Abismail, B., Canselier, J. P., Wilhelm, A. M., Delmas, H. Gourdon, C., 1999, Emulsification by ultrasound: drop size distribution and stability, *Ultrasonics Sonochemistry*, 6, 75-83.
- Araujo, G. S., J.B.L. Matos, J.O., Fernandes, J.M. Cartaxo, R.B. Goncalves, A.N. Fernandes, R.L. Farias, 2013, Extraction of lipids from microalgae by ultrasound application: prospection of the optimal method, *Ultrasonics Sonochemistry*, 20, 95-98 .
- Bonnet, D., Barthès, M., Girardot, L. and Bailly, Y., 2011, PYV: A PIV processing software in Python, proc. of Euroscopy, Paris, France.
- Bonnet, D., Barthès, M., Girardot, L. Bailly, Y., 2012, Simultaneous PIV measurements in the intake manifold's runners of a running automotive engine, proc. of 15th International Symposium on Flow Visualization, Minsk, Belarus.
- Gondrexon, N., Renaudin, V., Clément, M., Boldo, P., Pétrier, C., Gonthier, Y., Bernis, A., (1995) Récents Progrès en Génie des Procédés, 9, 41, 71-76
- Hihn J.Y., Doche M.L., Mandroyan A., Hallez L., Pollet B.G., 2011, Respective contribution of cavitation and convective flow to local stirring in sonoreactors, *Ultrasonics Sonochemistry*, 18, 881-87.
- Mazue, G., Viennet, R., Hihn, J.Y., Carpentier, L., Devidal, P., Albaina, I., 2011, Large-scale ultrasonic cleaning system: Design of a multi-transducer device for boat cleaning (20 kHz), *Ultrasonics Sonochemistry*, 18, 895-900.
- Mazue, G, Viennet, R, Hihn, J Y. (2013). "Transport limited current for equivalent flow velocity determination in simultaneous presence of ultrasound and tangential flow". Submitted in *Ultrasonics Sonochemistry*.
- Mandroyan A., Viennet R., Bailly Y., Doche M. L. Hihn J.Y., (2009a), Modification of the ultrasound induced activity by the presence of an electrode in a sonoreactor working at two low frequencies (20 and 40kHz). Part I: Active zone visualization by laser tomography, *Ultrasonics Sonochemistry*, 16, 88-96.
- Mandroyan A., Doche M.L., Hihn J.Y., Viennet R., Bailly Y., Simonin L., 2009b, Modification of the ultrasound induced activity by the presence of an electrode in a sono-reactor working at two low frequencies (20 and 40kHz). Part II: Mapping flow velocities by particle image velocimetry (PIV), *Ultrasonics Sonochemistry*, 16, 97-104.
- Trabelsi, H.A. Lyazidi, J. Berlan, P.L. Fabre, H. Delmas, A.M. Wilhem, 1996, *Ultrasonics Sonochemistry*, 3, S125.

Pollet B.G., Hihn J.Y., Doche M.L., Lorimer J.P., Mandroyan A., Mason T.J., 2007, Transport limited currents close to an ultrasonic horn equivalent flow velocity determination, *Journal of the Electrochemical Society*, 154, E131-E38.

Raffel, M., Willert, C.E., Wereley, S.T., Kompenhans, J., 1998, *Particle image velocimetry, a practical guide*, Eds. Springer, Berlin.

Etude d'un champ ultrasonore de puissance (20kHz) au sein d'une circulation de liquide : application à un outil de nettoyage de coques de bateau in situ

MAZUE Gérald^{a, b}, VIENNET Rémy^b, HIHN Jean-Yves^b, BONNET Dimitri^{b, c}, BARTHES Magali^c,
BAILLY Yannick^c, ALBAÏNA Ignaki^a

^a Navyclean

Traverse Collet Redon, 13013 Marseille, France

^b Institut UTINAM (UMR UFC/CNRS 6213)

30 Avenue de l'Observatoire, 25000 Besançon, France

^c Institut FEMTO-ST (UMR UFC/CNRS 6174)

2 Avenue Jean Moulin, 90000 Belfort Cedex, France

Résumé

La présente étude s'inscrit dans le développement d'une station de lavage de coques de bateau in-situ automatisée et plus particulièrement dans la conception de sa tête de nettoyage intégrant 3 sonotrodes fonctionnant à 20kHz. Le déplacement de l'outil le long de la coque et l'aspiration intégrée des saletés décollées, en vue de leur récupération pour un traitement ultérieur, engendrent une circulation de fluide (perpendiculaire au champ) et introduisent de fortes perturbations. Pour notre application, il est important de vérifier que la qualité du nettoyage n'est pas affectée par ces perturbations. Un dispositif expérimental dédié a été conçu pour étudier l'influence d'une circulation de liquide perpendiculaire au champ ultrasonore. Deux techniques de caractérisations ont été utilisées pour l'observation et la quantification de ces interactions, la PIV et des mesures électrochimiques de transfert de matière.

Mots clés : nettoyage ultrasons, PIV, transfert de matière